Organic Semiconductors

DOI: 10.1002/anie.201409479

ortho-, *meta*-, and *para*-Dihydroindenofluorene Derivatives as Host Materials for Phosphorescent OLEDs**

*Maxime Romain, Sébastien Thiery, Anna Shirinskaya, Céline Declairieux, Denis Tondelier, Bernard Geffroy, Olivier Jeannin, Joëlle Rault-Berthelot, Rémi Métivier, and Cyril Poriel**

Abstract: *This work reports the first structure–properties relationship study of ortho [2,1-c]-, meta [1,2-a]-, and para [1,2-b]dihydroindenofluorenes, highlighting the influence of bridge rigidification on the electronic properties. This study has made it possible to devise an extended π-conjugated molecule with both a high triplet state energy level and excellent thermal and morphological stability. As a proof of concept, dihydroindenofluorenes were used as the host in sky-blue phosphorescent organic light-emitting diodes (PhOLEDs) with high performance.*

Structure–properties relationship studies of novel π-conjugated materials have resulted in the impressive development of organic electronics.[1] In this context, phenylene derivatives constitute an essential class of molecules that have been widely studied due to their high potential in organic electronics.[2] For example, the bridged *para*-terphenyl unit, namely 6,12-dihydroindeno[1,2-*b*]fluorene, is nowadays an important building block for organic light-emitting diodes (OLEDs),[2–4] organic field-effect transistors,[5] and even organic solar cells.[6] More recently, other positional isomers with different phenyl linkages (*para*/*meta*/*ortho*) and different ring bridging (*anti* versus *syn*) have started to appear in the literature[7–11] but they remain very scarce and are rarely introduced in electronic devices. In this context our group has, for example, recently reported the first incorporation of bridged *meta*-terphenyls, i.e. dihydroindeno[1,2-*a*]fluorene and dihydroindeno[2,1-*b*]fluorene, in nondoped blue OLEDs.[10] In another recent example, Haley et al. synthesized a new class of appealing electron-accepting materials based on an antiaromatic, fully conjugated [2,1-*c*]-indenofluorene backbone (bridged *ortho*-terphenyl).[7] However, the aromatic π-conjugated analogue, the dihydroindeno[2,1-*c*]fluorenyl core described in this work (incorporated in **3**, Scheme 1), is almost absent from literature[12–14]

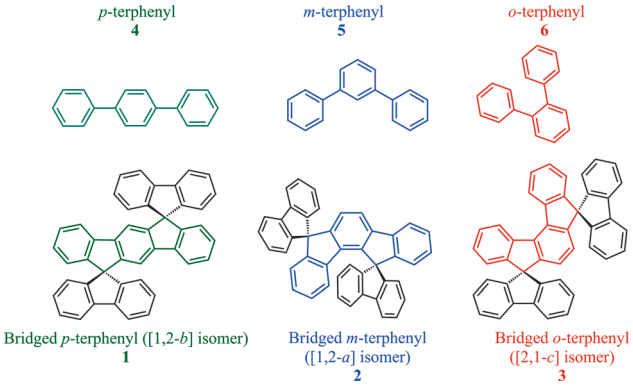

Scheme 1. Positional isomers of bridged *para*-, *meta*-, and *ortho*-terphenyls **1**–**3** (bottom) and their corresponding nonbridged counterparts **4**–**6** (top).

and its intrinsic properties have never been studied. Due to the importance of the dihydroindeno[1,2-*b*]fluorene in organic electronics, it is of great interest to design and incorporate the other dihydroindenofluorene isomers in other optoelectronic devices. For example, the design of organic host materials possessing a very high triplet state energy level ($E_T > 2.7$ eV)[15–19] represents a highly challenging task for the future of blue phosphorescent OLEDs (PhOLEDs). In this context, extended π-conjugated systems usually display a low E_T and dihydroindenofluorenes have hence never been studied for such applications.

Here we report the first structure–properties relationship study of structurally related bridged terphenyl isomers **1**–**3** (*para* [1,2-*b*]-, *meta* [1,2-*a*]-, and *ortho* [2,1-*c*]dihydroindenofluorenes; Scheme 1). When we compare them with the nonbridged terphenyl analogues **4**–**6** (Scheme 1) we find very unusual electronic properties induced by the bridge rigidification. We notably show that the linkages and bridges allow the fine-tuning of the electronic properties (mostly the energy level of the triplet state) of dihydroindenofluorenes. At the same time the excellent thermal and morphological stability essential to achieve stable electroluminescence in OLEDs can be maintained. Thanks to this control of the electronic and

[*] M. Romain, S. Thiery, Dr. O. Jeannin, Dr. J. Rault-Berthelot, Dr. C. Poriel
UMR CNRS 6226-ISCR-Université de Rennes 1
35042 Rennes cedex (France)
E-mail: cyril.poriel@univ-rennes1.fr
A. Shirinskaya, Dr. C. Declairieux, Dr. D. Tondelier, B. Geffroy
UMR CNRS 7647,LPICM-École Polytechnique
91128 Palaiseau (France)
B. Geffroy
LICSEN/IRAMIS/NIMBE, CEA Saclay
91191 Gif Sur Yvette (France)
Dr. R. Métivier
UMR CNRS 8531-PPSM, ENS Cachan
94235 Cachan (France)

[**] We thank the CDIFX and CRMPO (Rennes), CINES (Montpellier), ISA (Villeurbanne), Region Bretagne, and ADEME for a scholoarship (M.R.) and the ANR (no. 11-BS07-020-01) for scholarships (S.T., C.D., and A.S.). OLED = organic light-emitting diode.
Supporting information for this article is available on the WWW under http://dx.doi.org/10.1002/anie.201409479.

physical properties, we were able to obtain an organic semiconductor, namely **2**, possessing not only a very high triplet state energy level (2.76 eV), one of the highest recorded for pure hydrocarbon derivatives,[17,20–22] but also excellent thermal stability. The three isomers **1**–**3** have been successfully introduced as hosts in green (tris(2-phenylpyridine)iridium, $Ir(ppy)_3$), and sky-blue (bis[2-(4,6-difluorophenyl)pyridinato-*C2*,*N*](picolinato)iridium(III), FIrpic) PhOLEDs with high performance. We are reporting, to the best of our knowledge, the first example of a dihydroindenofluorene used as the host in a sky-blue PhOLED.

The syntheses of dispiro[fluorene-9,12′-indeno[1,2-*b*]-fluorene-7′,9″-fluorene (**1**, bridged *p*-terphenyl),[4] dispiro-[fluorene-9,11′-indeno[1,2-*a*]fluorene-12′,9″-fluorene] (**2**,[10] bridged *m*-terphenyl), and dispiro[fluorene-9,5′-indeno[2,1-*c*]fluorene-8′,9″-fluorene] (**3**, bridged *o*-terphenyl) are described in the Supporting Information.

The first oxidation potentials of compounds **1** and **2** were recorded at 1.43 V[10] and 1.57 V[23] (versus the standard calomel electrode, SCE), respectively, leading to HOMO levels of −5.76 eV and −5.86 eV (HOMO (eV) = $-[E_{onset}{}^{ox} + 4.4]$, based on an SCE energy level of 4.4 eV relative to vacuum (see the Supporting Information). The fact that the HOMO energy level of **2** is lower than that of **1** may be directly related to the different phenyl–phenyl linkages (**1**: *para*; **2**: *meta*) which make the π-conjugation pathway in **2** shorter than that in **1**. Indeed, an inspection of the shape of the HOMO of **1** reveals that the electron density is delocalized through the three phenyl units, whereas in **2** we note an interruption of the π-conjugation at the two opposite carbon atoms of the central phenyl ring (nodal plane), leading to weak electron density on the external phenyl rings (Figure 1). In this way, isomer **2** bears a strong resemblance to the fluorene molecule (HOMO = −5.88 eV[4]). Surprisingly, the HOMO level of **3** lies at −5.87 eV, almost identical to that of **2**. However, the shape of the HOMO of **3** is noticeably different from those of **1** and **2**. Indeed, the electron density of the HOMO of **3** is mainly located on the fluorenes with also a contribution on the central phenyl ring of the dihydro[2,1-*c*]indenofluorenyl core (Figure 1). In addition, we note in **3** the existence of a very close (almost degenerate) HOMO−1 energy level, in which the electron density extends exclusively along the dihydro[2,1-*c*]indenofluorene unit (see the Supporting Information). If one considers the character of its HOMO, **3** also resembles a fluorene molecule (as stressed for **2**) despite the fact that we may have expected a more conjugated terphenyl backbone (*ortho* versus *meta* linkages).[24–26] It seems that the π-conjugation restriction of **3** surely imposed by the *ortho–ortho* phenyl linkage is caused by the deformation of the dihydro[2,1-*c*]indenofluorenyl core (dihedral angle of 13° between the two external phenyl rings, see its helicene structure in the Supporting Information). As a result, the energy levels of the HOMO and HOMO−1 are inverted compared to the molecular orbitals of the "classical" dihydro[1,2-*b*]indenofluorene.

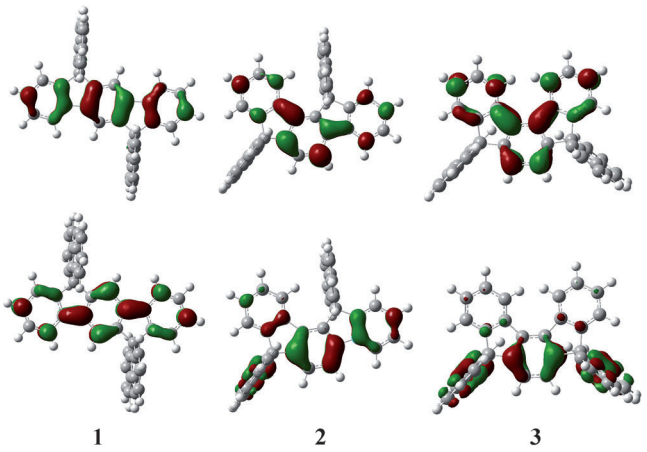

Figure 1. DFT-calculated frontier molecular orbitals of **1**–**3** (top: HOMO; bottom: LUMO) after geometry optimization at the B3LYP/6-311G + (d,p) level (isovalue: 0.04).

Through cathodic explorations, the LUMO levels of **1**–**3** were evaluated at −2.17 eV, −1.70 eV, and −2.00 eV, respectively (Table 1). Theoretical calculations provide a similar trend, with the LUMO of **2** (−1.38 eV) being higher in energy than the LUMOs of **1** (−1.56 eV) and **3** (−1.59 eV). A different trend was observed for the HOMOs (see above). Thus, the HOMO and LUMO of **3** present a different character (electron density of the HOMO mainly located on the fluorenes and electron density of the LUMO located on the dihydroindenofluorene), whereas for **2** (and **1**) the electron densities of both HOMO and LUMO are spread on the dihydroindenofluorenyl core. This feature clearly indicates the different influence of the linkages on the HOMO and LUMO levels.

The UV/Vis absorption and fluorescence spectra of **1**–**3** and of the corresponding nonbridged *para*-, *meta*-, and *ortho*-

Table 1: Electronic data of **1**–**6**.

		1	**2**	**3**	**4**	**5**	**6**
λ_{abs} (ε) [nm][a]		344	343	338	277	246	279
($\times 10^4$ L mol^{-1} cm^{-1})		(3.48)	(0.06)	(0.5)	(3.16)	(3.61)	(0.25)
			334				233
			(0.1)				(2.91)
λ_{em} [nm][a]		346	342	343	325	325	358
		365	355	358	339	339	
HOMO [eV]	el[b]	−5.76	−5.86	−5.87	−5.96	−6.04	−6.07
	calc[d]	−5.68	−5.8	−5.93	−6.13	−6.32	−6.27
LUMO [eV]	el[b]	−2.17	−1.70	−2.00	−2.00	−1.91	−1.89
	calc[d]	−1.56	−1.38	−1.59	−1.4	−1.25	−1.14
ΔE [eV]	opt[c]	3.53	3.53	3.60	4.03	4.43	4.23
	el[b]	3.59	4.16	3.87	3.96	4.13	4.18
	calc[d]	4.12	4.42	4.34	4.44	5.07	5.14
E_T [eV]	opt[e]	2.52	2.76	2.63	2.55[f]	2.82[f]	2.67[f]
	calc[d]	2.55	2.81	2.67	2.67	2.98	2.87
T [s][e]		2.6	5.5	2.2	–	–	–
EQE [%][g]	$Ir(ppy)_3$	9.9	14.8	13.3	3.8	–	–
	FIrpic	–	7.5	–	–	–	–

[a] In cyclohexane. [b] From redox data. [c] From UV/Vis spectra in cyclohexane. [d] At B3LYP/6-311G + (d,p) level of theory. [e] At 77 K in methylcyclohexane/2-methylpentane (1:1). [f] From Ref. [15]. [g] Maximum value with $J \geq 1$ mA cm^{-2}.

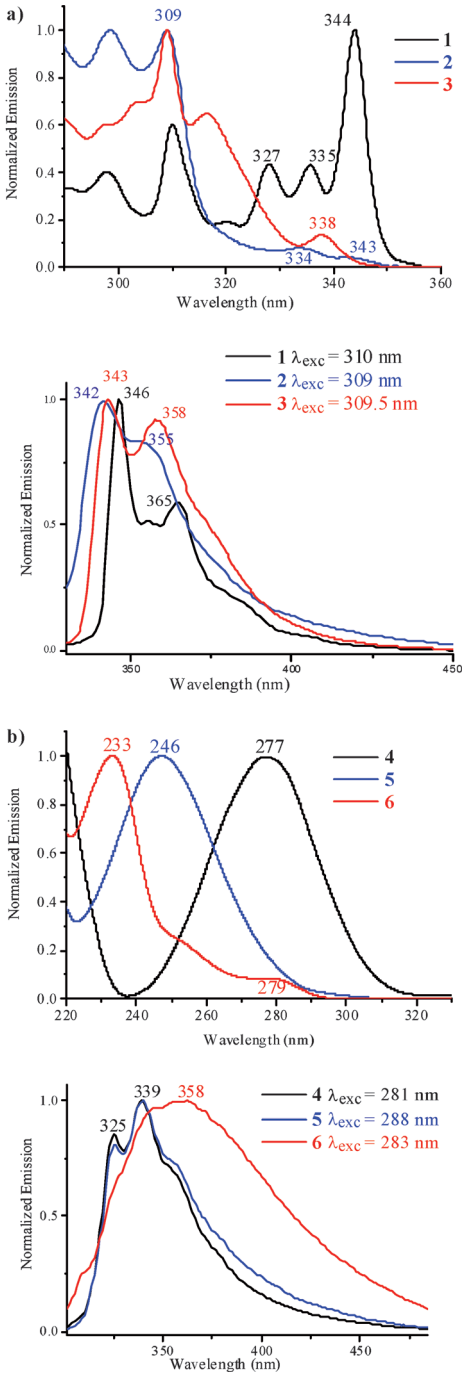

Figure 2. UV/Vis absorption and emission spectra (cyclohexane) of bridged terphenyls a) **1**–**3** and b) nonbridged terphenyls **4**–**6**.

terphenyls **4**–**6** are presented in Figure 2 (see also Table 1). In cyclohexane, **1**–**3** surprisingly present almost identical low-energy absorption maxima (344 nm for **1**, 343 nm for **2**, and 338 nm for **3**), with nevertheless an impressive difference in the intensity of the lowest-energy absorption band (**1**: $\varepsilon_{344nm} = 4.8 \times 10^4\,L\,mol^{-1}\,cm^{-1}$, **2**: $\varepsilon_{343nm} = 0.06 \times 10^4\,L\,mol^{-1}\,cm^{-1}$, and **3**: $\varepsilon_{338nm} = 0.5 \times 10^4\,L\,mol^{-1}\,cm^{-1}$). This weakness of this band in **2** and **3** seems to be unique to these dihydroindenofluorenes.[10] Indeed, other dihydroindenofluorenes ([1,2-*b*], [2,1-*a*], [2,1-*b*]) all display high molar absorption coefficients. This singular behavior of **2** and **3** may be related to symmetry considerations induced by the position of the bridge on the dihydroindenofluorenyl core. In addition and unlike the [2,1-*b*], [1,2-*b*], and [2,1-*a*] regioisomers, **2** and **3** have strained structures leading to a deformation of the dihydroindenofluorenyl cores (10° for the [1,2-*a*] isomer[10] and roughly 13° for the [2,1-*c*] isomer, see the crystal structure in the Supporting Information). Such structural aspects may also have an influence on the partially allowed/forbidden nature of the first electronic transitions. In time-dependent density functional theory (TD-DFT) calculations (see the Supporting Information), we indeed note that in **1** the main π–π* transition is a HOMO/LUMO transition associated with a very high oscillator strength (0.4617). In contrast, the HOMO–LUMO transitions of **2** and **3** have weak oscillator strengths (0.0231 and 0.0291), the major π–π* transition being shifted to higher energies.

The absorption spectra of the nonbridged terphenyls **4**–**6** are drastically different from those of their bridged analogues **1**–**3** (Scheme 1). Indeed, absorption spectra of **4**–**6** display maxima at 277 nm, 246 nm, and 233/279 nm, respectively (Table 1). First, there is an impressive red shift of the absorption maxima between **1**–**3** and **4**–**6**, attributed to the presence of the bridges in **1**–**3**. Indeed, the molecular structures of **1**–**3** avoid any torsion between the phenyl linkages responsible for interruption of the π-conjugation, as seen, for example, in the case of *ortho* terphenyl **6**. Indeed, **6** presents two absorption bands, one very intense at 233 nm and one very weak at 279 nm. This last band is analogous to that of the *para* isomer **4**, thus indicating a minor proportion of conformers of **6** with a more planar structure and a certain degree of π-conjugation between the phenyl units. TD-DFT calculations indicate that the first transition wavelengths ($\lambda_{max} = 286$ nm for **4**, 263 nm for **5**, and 271 nm for **6**) are in accordance with experimental results (Table 1), following a clear *para*/*ortho*/*meta* sequence and corresponding to HOMO/LUMO transitions (see the Supporting Information). Thus, the presence of the bridges (and the induced rigidification) in **2** and **3** significantly changes the nature of the main transition compared to that of the nonbridged analogues **5** and **6** (which is not the case for **1** and **4**). This is a peculiar result of the bridge effect in dihydroindenofluorenes.

An important feature is the optical energy gaps ΔE_{opt} of **1**–**3**, which are almost identical, ranging from 3.53 eV for **1** and **2** to 3.60 eV for **3**, and hence different from those from the electrochemical analyses. This feature is highly surprising since the nonbridged analogues **4**–**6** present very different ΔE_{opt} values (4.03 eV, 4.43 eV, and 4.23 eV, respectively) clearly dependent on the nature of the phenyl linkages. As mentioned above, it is usually accepted that there is a better delocalization of π-electrons following the *para*/*ortho*/*meta* sequence, and a number of studies have tried to elucidate the origin of the restriction in the π-conjugation between *para*- and *meta*-substituted oligophenylenes.[24–26] Thus, Hogen-Esch et al. have invoked a shorter π-conjugation pathway to explain the blue shift in the absorption spectra of a series of *meta*-linked fluorenes compared to their *para* analogues.[26] In our case, the torsion angle seems also to play a major role in the restricted π-conjugation as there is no difference in the

ΔE_{opt} values of **1**–**3**, whereas terphenyls **4**–**6** possess different ΔE_{opt} values. Thus, the rigidification of the three terphenyl units in **1**–**3** eliminates the effect of the linkages on the optical energy gap. The properties of **1**–**3** in their excited state strengthen this hypothesis (see below).

The emission spectra of **1**–**3** are well resolved and very similar, with maxima at 346 nm for **1**, 342 nm for **2,** and 343 nm for **3** (Figure 2). Similarly, the fluorescence spectra of **4** and **5** have maxima at 325 nm and 339 nm which are surprisingly similar in shape and wavelength (Figure 2). The Stokes shift, notably that of **5**, appears very large (48 nm for **4** and 79 nm for **5**). There is hence a clear breakdown of the mirror-image symmetry in the absorption/emission spectra of **4** and **5**. Heimel et al. previously reported this feature for *para*-terphenyl **4**,[27] arising from its planarization in the excited state and a strong reorganization energy. They notably correlated the degree of torsional freedom found in **4** and the breakdown of the mirror image.[27] Herein, *meta*-terphenyl **5** obeys similar rules and hence **4** and **5**, in the excited state, interestingly possess identical spectra, independent of the nature of the linkage. It should be stressed that *ortho*-terphenyl **6** presents a different spectrum with a large and red-shifted band assigned to an intramolecular excimer emission due to through-space interactions between the two nonlinked phenyl rings that avoid planarization in the excited state. Remarkably, we note a strong similarity in the emission spectra for bridged terphenyls **1** and **2** and their nonbridged analogues **4** and **5**, whereas their absorptions were noticeably different. Thus, the planarization of **4** and **5** in the excited state leads to a geometry that can be compared to that of **1** and **2**, which are already planarized by the bridges in the ground state, with surely a weak reorganization energy (in accordance with the small Stokes shift). This remarkable feature caused by the bridges negates the effect of the linkages on the optical properties and may explain the similar ΔE_{opt} values and emission spectra of **1**–**3**.

At 77 K, the emission spectra of **1**–**3** present a well-resolved phosphorescence contribution, constituted of two maxima recorded at 490 and 531 nm for **1**, 448 and 482 nm for **2,** and 471 and 507 nm for **3** (see the Supporting Information). The corresponding E_T values of **1**–**3**, obtained from the highest-energy phosphorescence peak, were thus estimated at roughly 2.52, 2.76, and 2.63 eV, respectively, in accordance with theoretical calculations (Table 1). Due to the π-conjugation disruption, the triplet state energy level of the *meta*-substituted terphenyl **2** is remarkably higher than that of the *para*-substituted terphenyl **1**. Due to its *ortho* linkages, **3** possesses a E_T value intermediate to those of **1** and **2**. Nonbridged terphenyls **4**–**6** display E_T values of 2.55, 2.82, and 2.67 eV respectively,[15] following the same trend as that discussed above. Thus, and in contrast to our observations in UV/Vis absorption and fluorescence spectroscopy, the nature of the linkage fully determines the E_T values. Thus, *para*-substituted derivatives **1** and **4** possess almost identical E_T values and hence a similar location of the triplet state. The same conclusion can be drawn for *meta*-substituted derivatives **2** and **5**, and *ortho*-substituted derivatives **3** and **6**. Indeed, the electron density of the frontier molecular orbitals involved in the triplet excited state of *para*-substituted oligophenyls is delocalized along the longest molecular axis, while that of *meta*-substituted oligophenyls is localized in each biphenyl component.[15] Bridged terphenyls **1**–**3** seem to display an identical behavior and hence singlet and triplet state energy levels follow different trends. This makes it possible to tune the triplet state energy level without modifying that of the singlet state. Finally, radiative deactivation of the triplet state of **1**–**3** is very slow. Phosphorescence decay was measured and the lifetime of the T_1 state of **1** and **3** was found to be (2.6 ± 0.1) s and (2.2 ± 0.1) s, respectively. The *meta* linkages of **2** have an important influence on the photophysical properties of the triplet state, since its lifetime ((5.5 ± 0.3) s) was found to be twice as long as that of the *para*/*ortho* isomers, highlighting the impact of the nature of the linkages on the phosphorescence lifetimes.

In order to confirm the efficiency of the present chemical design, we studied **1**–**6** by thermogravimetric analysis (TGA) and differential scanning calorimetry (DSC) (see the Supporting Information). Due to the presence of the rigid spiro bridges, **1**–**3** are highly thermally stable with 5% mass loss occurring at 355, 330, and 347 °C, respectively, whereas this mass loss occurs at much lower temperatures for **4**–**6** (**4**: 176 °C, **5**: 151 °C, **6**: 123 °C). Thus, this mass loss attributed to sublimation is weakly dependent on the phenyl linkages in **1**–**3**, but strongly dependent on them in **4**–**6**. In addition, no significant phase transition (melting, crystallization, glass transition) was detected for **1**–**3** by DSC (between 20 and 300 °C). Such thermal behavior is of great importance to improve the lifetime of OLEDs. Terphenyls **4**–**6** present drastically different properties (see the Supporting Information) with, for example, a very low melting transition observed for **5** (85 °C) and **6** (55 °C), and for **5** even a sharp crystallization at a very low temperature (35 °C); thus terphenyls **4**–**6** are not suitable for device application (see below). Thus, the physical properties of **2** are much better than those of its nonbridged analogue **5**, though the high E_T is maintained.

In order to explore the potential of the present dihydroindenofluorenes as hosts for phosphorescent dopants, we fabricated green ($Ir(ppy)_3$, $E_T = 2.42$ eV)[15] and sky-blue (FIrpic, $E_T = 2.64$ eV)[15] PhOLEDs. The best performance of green PhOLEDs has been recorded with **2** as the host doped with 10 wt% of $Ir(ppy)_3$ (see the Supporting Information). The device emits light at a low voltage of 2.8 V, with a maximum current efficiency (CE) as high as 57.3 cd A^{-1}, a maximum power efficiency (PE) of 30.3 Lm W^{-1}, and an external quantum efficiency (EQE) of 14.8%. The performance of the two other isomers as hosts appears to be poorer than that of **2**, maybe due to their lower E_T values, but they are nevertheless efficient (**1**: CE = 31.4 cd A^{-1}, PE = 15.5 Lm W^{-1}, EQE = 9.9%; **3**: CE = 49.0 cd A^{-1}, PE = 26.6 Lm W^{-1}, EQE = 13.3%; see the Supporting Information). With a CE of roughly 57.3 cd A^{-1}, green devices using **2** as the host appear to be among the highest obtained with pure hydrocarbons.[3,21,22] These results indicate that dihydroindenofluorenes enable PhOLEDs to efficiently function at low operating voltages. More importantly, **2** has been used as a host for the well-known sky-blue or greenish blue FIrpic emitter (25%) in a similar device configuration. Thus, FIrpic-

based PhOLEDs present a maximum CE of 21.1 cd A^{-1}, PE of 11.9 Lm W^{-1}, EQE of 7.5 %, and a very low threshold voltage (3.2 V); the electroluminescent spectrum (see the Supporting Information) displays exclusively the emission of FIrpic, meaning that the energy-transfer cascade is efficient. Compared to other structurally related pure hydrocarbon hosts previously reported in literature, such as 4-phenylspirobifluorene (EQE = 5.7 %)[22] and spirobifluorene (EQE = 6.6 %),[22] and using exactly the same device architecture, we note that FIrpic-based devices using **2** as the host are more efficient. This high performance indicates a good confinement of the triplet excitons and appears remarkable for a PhOLED based on a molecule with an extended π-conjugated backbone, which is usually incapable of efficient energy transfer since its E_T is too low.

In order to highlight the efficiency of the strategy based on bridged terphenyls developed herein, we have investigated benchmark devices using nonbridged terphenyls **4**–**6**. However, due to their physical properties, deposition of **5** and **6** under reduced pressure and even at low temperatures appears to be impossible and no device can be fabricated with these materials. Terphenyl **4** was amenable to deposition and a 10 wt % $Ir(ppy)_3$ doped device has been fabricated and characterized. The performance appears nevertheless very low with an EQE of 3.8 % (see the Supporting Information), around four times lower than that recorded for **2**. These findings clearly indicate the efficiency of the "bridging approach" and the potential of dihydroindenofluorenes as hosts for PhOLEDs.

To summarize, this work reports the first structure–properties relationship study of *ortho* [2,1-*c*]-, *meta* [1,2-*a*]-, and *para* [1,2-*b*]dihydroindenofluorenes, highlighting the influence of the bridge rigidification on the electronic properties. The simple molecular design investigated in this work makes it possible to devise extended π-conjugated molecules having both a high E_T value and excellent thermal/morphological stabilities. The proof of concept has been demonstrated through the first use of dihydroindenofluorenes as the host in a sky-blue PhOLED.

Received: September 25, 2014
Published online: December 2, 2014

Keywords: dihydroindenofluorenes · LEDs · organic semiconductors

[1] Thematic issue: π-Functional Materials (Eds.: J. L. Bredas, S. R. Marder, E. Reichmanis), *Chem. Mater.* **2011**, *23*, 309.
[2] A. C. Grimsdale, K. Müllen, *Macromol. Rapid Commun.* **2007**, *28*, 1676.
[3] L.-C. Chi, W.-Y. Hung, H.-C. Chiu, K.-T. Wong, *Chem. Commun.* **2009**, 3892.
[4] C. Poriel, J.-J. Liang, J. Rault-Berthelot, F. Barrière, N. Cocherel, A. M. Z. Slawin, D. Horhant, M. Virboul, G. Alcaraz, N. Audebrand, L. Vignau, N. Huby, G. Wantz, L. Hirsch, *Chem. Eur. J.* **2007**, *13*, 10055.
[5] H. Usta, C. Risko, Z. Wang, H. Huang, M. K. Deliomeroglu, A. Zhukhovitskiy, A. Facchetti, T. J. Marks, *J. Am. Chem. Soc.* **2009**, *131*, 5586.
[6] Q. Zheng, B. J. Jung, J. Sun, H. E. Katz, *J. Am. Chem. Soc.* **2010**, *132*, 5394.
[7] A. G. Fix, P. E. Deal, C. L. Vonnegut, B. D. Rose, L. N. Zakharov, M. M. Haley, *Org. Lett.* **2013**, *15*, 1362.
[8] A. Shimizu, Y. Tobe, *Angew. Chem. Int. Ed.* **2011**, *50*, 6906; *Angew. Chem.* **2011**, *123*, 7038.
[9] A. Shimizu, R. Kishi, M. Nakano, D. Shiomi, K. Sato, T. Takui, I. Hisaki, M. Miyata, Y. Tobe, *Angew. Chem. Int. Ed.* **2013**, *52*, 6076; *Angew. Chem.* **2013**, *125*, 6192.
[10] M. Romain, D. Tondelier, J.-C. Vanel, B. Geffroy, O. Jeannin, J. Rault-Berthelot, R. Métivier, C. Poriel, *Angew. Chem. Int. Ed.* **2013**, *52*, 14147; *Angew. Chem.* **2013**, *125*, 14397.
[11] D. Thirion, C. Poriel, R. Métivier, J. Rault-Berthelot, F. Barrière, O. Jeannin, *Chem. Eur. J.* **2011**, *17*, 10272.
[12] Y.-Y. Li, H.-Y. Lu, M. Li, X.-J. Li, C.-F. Chen, *J. Org. Chem.* **2014**, *79*, 2139.
[13] Y. Shi, Q. Liu, G. Wu, L. Rong, J. Tang, *Tetrahedron* **2011**, *67*, 1201.
[14] B. Du, L. Wang, S.-C. Yuan, T. Lei, J. Pei, Y. Cao, *Polymer* **2013**, *54*, 2935.
[15] H. Yersin, *Highly Efficient OLEDs with Phosphorescent Materials*, Wiley-VCH, Weinheim, **2007**.
[16] L. Xiao, Z. Chen, B. Qu, J. Luo, S. Kong, Q. Gong, J. Kido, *Adv. Mater.* **2011**, *23*, 926.
[17] Y. Tao, C. Yang, J. Qin, *Chem. Soc. Rev.* **2011**, *40*, 2943.
[18] Z.-S. Zhang, Z. Zhang, R. Chen, J. Jia, C. Han, C. Zheng, H. Xu, D. Yu, Y. Zhao, Y. Pengfei, S. Liu, W. Huang, *Chem. Eur. J.* **2013**, *19*, 9549.
[19] K. S. Yook, J. Y. Lee, *Adv. Mater.* **2012**, *24*, 3169.
[20] S. Ye, Y. Liu, C.-a. Di, H. Xi, W. Wu, Y. Wen, K. Lu, C. Du, Y. Liu, G. Yu, *Chem. Mater.* **2009**, *21*, 1333.
[21] C. Fan, Y. Chen, P. Gan, C. Yang, C. Zhong, J. Qin, D. Ma, *Org. Lett.* **2010**, *12*, 5648.
[22] S. Thiery, D. Tondelier, C. Declairieux, G. Seo, B. Geffroy, O. Jeannin, J. Rault-Berthelot, R. Métivier, C. Poriel, *J. Mater. Chem. C* **2014**, *2*, 4156.
[23] C. Poriel, J. Rault-Berthelot, D. Thirion, *J. Org. Chem.* **2013**, *78*, 886.
[24] S. Karabunarliev, M. Baumgarten, N. Tyutyulkov, K. Müllen, *J. Phys. Chem.* **1994**, *98*, 11892.
[25] S. Y. Hong, D. Y. Kim, C. Y. Kim, R. Hoffmann, *Macromolecules* **2001**, *34*, 6474.
[26] N. Fomina, S. E. Bradforth, T. E. Hogen-Esch, *Macromolecules* **2009**, *42*, 6440.
[27] G. Heimel, M. Daghofer, J. Gierschner, E. J. W. List, A. C. Grimsdale, K. Müllen, D. Beljonne, J. L. Brédas, E. Zojer, *J. Chem. Phys.* **2005**, *122*, 054501.

